

INVESTIGATION OF ATMOSPHERIC INSTABILITY FOR COMMUNICATION EXPERIMENTS WITH THE ESA'S GEOSTATIONARY SATELLITE ARTEMIS

V. Kuz'kov¹, V. Andruk¹, Yu. Sizonenko¹, Z. Sodnik²

¹*Main Astronomical Observatory, NAS of Ukraine
27 Akademika Zabolotnoho Str., 03680 Kyiv, Ukraine
e-mail: kuzkov@mao.kiev.ua*

²*ESTEC (European Space Research and Technology Centre)
ESA, Postbus 229, 2200 AG Noordwijk, The Netherlands*

The investigations of the atmospheric turbulence instability are carried out. The observations of different stars and different positions of stars in the sky performed with the AZT-2 telescope (diameter of 0.7 m) of the Main Astronomical Observatory, Kyiv, Ukraine, and at the Optical Ground Station (the 1.0-m telescope) of ESA at Canary Islands are described. Short exposures (40 ms) with CCD cameras in focal plane of objectives with the filters were used. The calculations of middle positions of star images were performed. The deviation of star's image positions from the middle position was also performed. The atmospheric attenuation and *FWHM* (Full Width Half Maximum) function were calculated using the MIDAS/ROMAFOT software package. The results of analyses of experimental data obtained due to observations in different regions are also presented.

INTRODUCTION

Free-space laser communication systems can achieve very high data rates in comparison with radio communication systems, especially on deep-space distances. This complicated and mastered technology has been proved by European Space Agency (ESA) in the world-first inter-satellite laser communication link between its geostationary satellite ARTEMIS and the low Earth orbiting satellite SPOT-4 [5]. Laser communication experiments are also being performed between ARTEMIS and the ESA's Optical Ground Station (OGS) at Tenerife, Spain [4].

ARTEMIS is a telecommunication demonstration satellite in geostationary orbit, positioned 21.5 degrees East.

After matching calculations we showed that the same experiments of receiving-transmitting the information by laser communication channel can be performed by using common astronomical telescopes. A meeting of the representatives of ESA and the Main Astronomical Observatory (MAO) was held in June 2002 in Kyiv. According to the meeting protocol, MAO can plan a laser communication link experiment between ESA's ARTEMIS satellite and the MAO's telescopes (optical ground-based station) in Kyiv. After this meeting, MAO started to prepare the laser communication link experiment with ARTEMIS [2, 3]. This will enable comparisons of the laser beam propagation across the atmosphere in different regions, in particular, between the Atlantic region (Canary Islands) and the continental region (Ukraine).

Investigations of atmospheric instabilities, in particular atmospheric attenuation and turbulence, are very important for the ground-satellite laser propagation to determine an optimum beam divergence of the laser power.

EXPERIMENTAL METHOD

The laser wavelengths used by ARTEMIS are 815–825 nm for the downlink and 843–853 nm for the uplink. The divergence of the laser beam is approximately 1 arcsec, but atmospheric turbulence is strongly influencing the laser beam propagation and the power density of laser radiation. It is interesting to compare atmospheric instabilities between the OGS at an altitude of $h = 2400$ m above sea level and the telescope of MAO at an altitude of $h = 175$ m above sea level (Kyiv).

For a first estimation of atmospheric instabilities, observations of standard stars were performed at elevation angles (air mass) similar to ARTEMIS. Common observations were performed with the guider telescope

($F = 2.5$ m, $D_{in} = 0.2$ m) of the 0.7-m AZT-2 telescope at MAO, Kyiv using a TV format CCD camera (Chiper Cam CPT-CDH70) and with the Coude CCD camera (Astro Cam 4202) at the 1-m OGS telescope ($F_{ef} = 11$ m) at the Teide Observatory, Tenerife, Canary Islands.

The technical data of the CCD cameras are shown in Table 1.

Table 1. The technical data of the CCD cameras

CCD camera	Sensor	Pixels	Pixel size, μm	FOV per pixel arcsec	Used filter
CPT-CDH70	Sony	795×596	8.6×8.3	0.72×0.69	850 nm, $\Delta\lambda = 10$ nm
VersArray 1300F	E2V CCD36-40	1340×1300	20.0×20.0	0.42×0.42	530–635 nm

The length of exposure was 40 ms with a 1 s time interval between exposures.

An example of a stellar image (α Aql) obtained with the “Sony” CCD sensor is shown in Fig. 1.

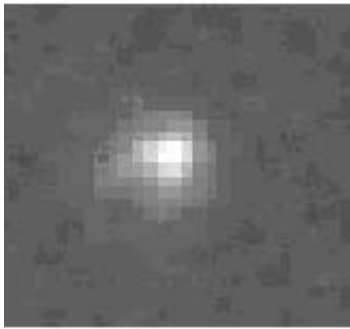


Figure 1. Image of star α Aql

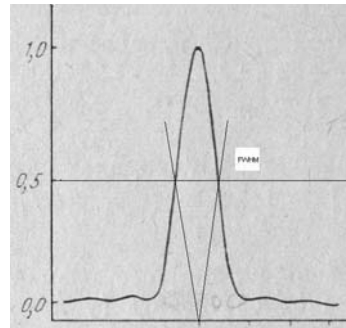


Figure 2. *FWHM* function

MEASUREMENT AND CALCULATION RESULTS

It is well known that the resolution of a telescope does not reach the diffraction limit by ground observations because of atmospheric turbulence. The achievable resolution limit is dependent on the location of observation site and for good sites it is about one arcsec without the use of adaptive optics. Atmospheric turbulence leads to scintillation and image motion in the focal plane of the telescope. Image motion is caused by varying angles by arriving a plane wave front. Scintillations are caused by brightness variations of stellar images and blurring is caused by stellar diameter variations resulting from focusing or defocusing of the stellar light.

It is possible to retrieve information about atmospheric turbulence conditions from short-exposure images of point sources (stars) in focal plane. A list of observed stars is given in Table 2.

Table 2. List of observed stars

Star	V	UT	LST	A (S)	Z	X
5276	6.39 ^m	04/04 – 25. ^d 91939	12 ^h 25 ^m 20 ^s	320.86°	41.24°	1.326
α Lnx	3.17	05/04 – 20.80764	13 20 09	175.09	46.75	1.454
α Oph	2.08	05/04 – 20.99653	17 52 54	12.31	38.37	1.273
α Aql	0.80	05/04 – 21.03125	18 43 02	342.95	42.81	1.359
β Aql	3.70	05/04 – 21.03819	18 53 03	345.57	44.97	1.409

LST – local star time; A – azimuth; Z – zenith angle; X – air mass.

The processing of the short exposure (40 ms) stellar CCD images were performed using the MIDAS/ROMAFOT software package [1]. The photometric calculations delivered the star magnitude M , the average

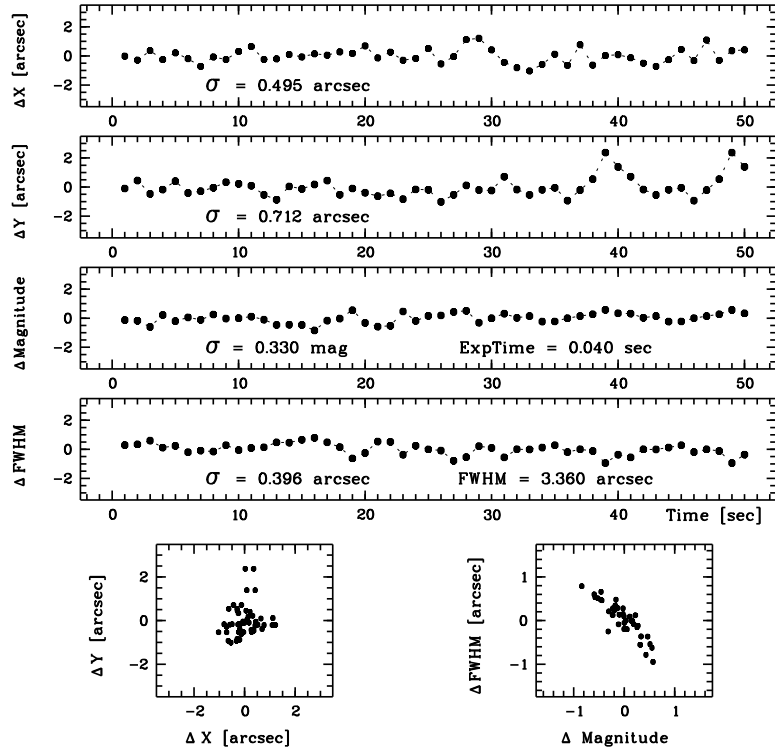


Figure 3. Result of processing of observations of star # 5276 at OGS ESA

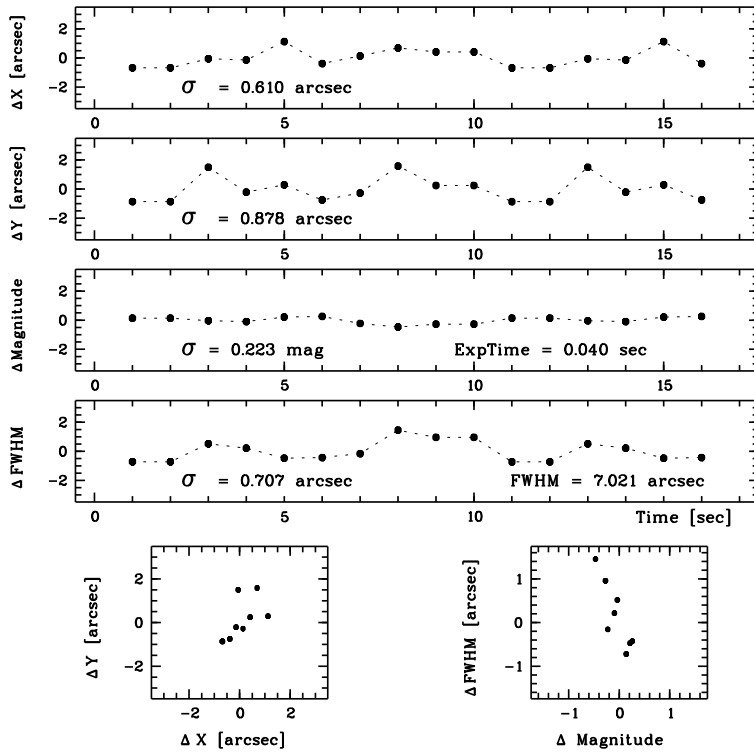


Figure 4. Result of processing of observations of star β Aql

star magnitude from N images, the deviation ΔM , and the standard root mean square (rms) deviation σ_{mag} . In addition, the calculations delivered the photometric center of every stellar image, the average photometric center position for N images, deviations Δx , Δy , and the standard root mean square deviation of the photometric center of stars from middle position in coordinate x and y (σ_x , σ_y).

For an estimation of scintillations or value of focusing of star images, the function Full Width Half Maximum ($FWHM$) was calculated, as example see Fig. 2. As a result, we get a deviation $\Delta FWHM$ and a root mean square deviation σ_{FWHM} .

The examples of calculation for stars from Table 2 are presented in Figs. 3 and 4.

The results of the summarized processing of the whole observational data are presented in Table 3.

Table 3. Results of the summarized processing of the whole observational data

Star	V	X	σ_{mag}	σ_x , arcsec	σ_y , arcsec	σ_{FWHM} , arcsec	N images
5276	6.39 ^m	1.326	0.330	0.495	0.712	0.396	50
α Lnx	3.17	1.454	0.246	1.049	0.662	0.623	16
α Oph	2.08	1.273	0.088	0.728	0.342	0.296	16
α Aql	0.80	1.359	0.065	0.498	0.812	0.241	16
β Aql	3.70	1.409	0.223	0.610	0.878	0.707	16

CONCLUSIONS

From analyses of experimental data and Figs. 3 and 4 one can see that there are no important differences between σ_x and σ_y data for the OGS site and the MAO site. The image motion in focal plane is a result of turbulence in higher altitude layers of the atmosphere (higher than 2400 m). The quality of images in the focal plane for long exposures is similar and equal to about 2 arcsec on the sky. It is, therefore, assumed that if the laser beam divergence in the future ground–space laser communication experiments with ARTEMIS is set to double the seeing value, namely 4 arcsec, and if the laser power is sufficient a fast and fine pointing and tracking mirror and control loop may not be necessary.

From Figs. 3–4 and Table 3 one can see that σ_{mag} for OGS observations is slightly greater than for MAO observations and can be determined by local time of observation. There is a difference of $\Delta FWHM / \Delta M$ values for observations at OGS and MAO too. $\Delta FWHM / \Delta M$ is equal to -1.108 for OGS observations. $\Delta FWHM / \Delta M$ is equal to -2.607 for β Aql and similar for another MAO observations. The difference of $\Delta FWHM / \Delta M$ values may be determined from differences of fields of view per pixel for various CCDs. To obtain more precise results, additional observations with similar focal length and filters are needed.

- [1] *Andruk V. N., Butenko G. Z., Ivashchenko Yu. N.* Processing of CCD images of star fields using the MIDAS/ROMAFOT software package // Kinematics and Physics of Celestial Bodies. Suppl. Ser.–2003, N 4.–P. 71–74.
- [2] *Kuz'kov V. P., Medvedskii M. M., Yatskiv D. Ya., et al.* Preparation for optical Communication Experiments with the Geostationary Satellite ARTEMIS // Space Sci. and Technology.–2003.–9, N 4.–P. 79–83.
- [3] *Kuz'kov V. P., Nedashkovskii V. N.* A Receiver with an Avalanche Photodiode for the Optical Communication Channel from a Geostationary Satellite // Instrum. and Exp. Techniques.–2004.–47, N 4.–P. 513–515.
- [4] *Reyes Garcia-Talavera M., Sodnik Z., Lopez P., et al.* Preliminary results of the in-orbit test of ARTEMIS with the Optical Ground Station // Proc. SPIE.–2002.–4635.–P. 38–49.
- [5] *Tolker-Nielsen T., Oppenhauser G.* In-orbit test result of an operational optical inter satellite link between ARTEMIS and SPOT4, SILEX // Proc. SPIE.–2002.–4635.–P. 1–15.